Within-Hand Manipulation Planning and Control for Variable Friction Hands

Gokul Narayanan[1], Joshua Amrith Raj[1], Abhinav Gandhi[1], Aditya A. Gupte[1], Adam J. Spiers[2], and Berk Calli[1(✉)]

[1] Robotics Engineering Department, Worcester Polytechnic Institute, Worcester, MA 01609, USA
{gsathyanarayanan,jcalebchanthiraj,agandhi2,aagupte,bcalli}@wpi.edu
[2] Department Haptic Intelligence, Max Planck Institute for Intelligent Systems, Stuttgart 70372, Germany
a.spiers@is.mpg.de

Abstract. In this work, we present three vision-based within-hand manipulation methods for a variable friction hand. The system is able to plan and execute actions such as in-hand sliding and large object rotation, which are required for many within-hand manipulation tasks. We present an experimental study using objects with various geometries, and show that all the methods can reliably achieve given target object poses. We discuss the advantages and disadvantages of the proposed methods with respect to positioning accuracy and efficiency.

1 Motivation, Problem Statement, Related Work

Humans heavily rely on their within-hand manipulation (WIHM) capabilities for performing their everyday activities [1]. These actions for re-orienting and re-positioning objects within hand help people streamline manipulation operations by achieving task-oriented hand-object configurations without the need for re-grasping (e.g. re-positioning a pen or a key after picking-up to make the objects ready for use). Controlled within-hand sliding and large object reorientation are two prominent actions that are frequently needed in WIHM, but are greatly

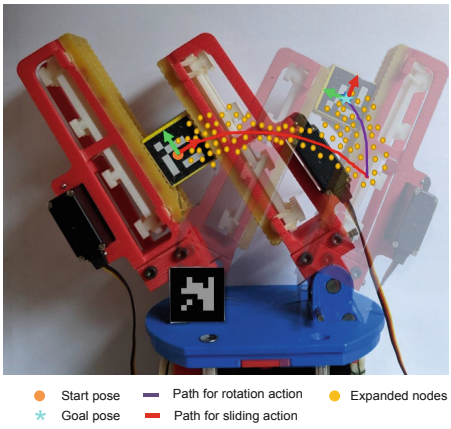

Fig. 1. WIHM from an arbitrary start pose to a desired pose via automatic planning and control using a variable friction hand.

G. Narayanan and J. A. Raj—Contributed equally to this publication.
This work was supported in part by the National Science Foundation under grant IIS-1900953.

B. Siciliano et al. (Eds.): ISER 2020, SPAR 19, pp. 600–610, 2021.
https://doi.org/10.1007/978-3-030-71151-1_53

challenging for robots even with sensorized, high-DOF, expensive hands operating in structured settings with accurate models [4,9,17].

In our previous work [14], we proposed a simple and open-source hand design that can change the effective friction of its finger surfaces to provide reliable within-hand sliding and large reorientation of a grasped object beyond the capabilities of the prior designs. These abilities were demonstrated with hard-coded actions and manual teleoperation. In this work, we expand on these abilities with the following additions (Fig. 1):

1. A generalized position and velocity-level kinematics model of the hand-object system that can work with arbitrary polygon objects,
2. Three novel approaches for conducting automatic WIHM:
   a. A feedforward control method based on a WIHM planner,
   b. A feedback control method using a visual servoing scheme,
   c. A hybrid method that combines the feedforward and feedback methods,
3. Experimental results using five objects with different shapes and sizes (in total 162 experiments),

We would like to clarify our assumptions and system properties for this current work as follows:

1. We only consider planar WIHM (object position and orientation in the grasp plane). While the variable friction mechanism can enable various 6D manipulation strategies, they are out of the scope of this paper.
2. Our system can operate with or without a support plane (i.e. when the object is lifted). All the presented experiments are without the support plane.
3. We assume that a geometric model of the object is provided. Nevertheless, this model does not need to be accurate since our feedback methods can compensate for modelling imperfections.
4. We assume that the target object has at least one flat surface to allow within-hand sliding.

Conventional WIHM methods (e.g. [12,13]) rely on accurate hand-object models, which are infeasible to obtain, whereas recent methods that relax this reliance via mechanical compliance [3] or impedance control [15] fail to achieve controlled sliding and large rotations. Our framework operates in the quasi-static level and provide reliable and precise WIHM without accurate hand-object models.

Dafle et al. [5] presented a method to perform within-hand manipulation via extrinsic dexterity by utilizing external contacts. Similarly the formulations in [13] perform controlled sliding via inertial forces and contacts with the environment. These methods, in addition to relying on the environment, also require accurate hand-object kinematics and dynamics models. In contrast, the variable friction hand does not rely on extrinsic contacts and can work with simple kinematic models with quasi-static assumptions, which greatly simplifies the planning and control approaches and boosts the system's robustness.

Finger-gaiting [15] is a method that uses three or more fingers to perform within-hand manipulation tasks without the use of extrinsic dexterity. However,

these approaches require sophisticated planning methods. The methods in [2,3] take advantage of the adaptive nature of the underactuated hands and utilize vision-based control schemes for achieving accurate WIHM. Nonetheless, these methods are limited to roling contacts.

Our hand with variable friction fingers [14] performs within-hand sliding and within-hand rotation of the object by leveraging the ability to change the friction properties of the fingers. As presented in this paper, using a simple kinematics model of the gripper system and a feedback loop control, we are able to perform within-hand manipulation tasks accurately and generalize to objects of different sizes and shapes. These methods are also applicable for recently developed mechanisms that were inspired by our design [10,11], or for similar systems such as [7,16].

2 Technical Approach

In this section, we briefly discuss the functionalities of the gripper, the kinematics model and the planning and control schemes we developed. Friction plays an important role in WIHM. Effective frictional forces between the finger and object surfaces can change the outcome of a particular finger motion on the object pose. The variable friction (VF) gripper is designed to alter the friction coefficients of the robotic fingers. Each finger can be set to a high friction or a low friction state. By setting the friction configuration appropriately, we are able to achieve various WIHM behaviours. As such, moving the fingers during the following friction conditions 1) $\{$*left finger*, *right finger*$\} = \{high, low\}$, 2) $\{low, high\}$ and 3) $\{high, high\}$ leads to 1) sliding of the object along the right finger, 2) sliding of the object along the left finger and 3) rotating the object. For the hand's working principles, please refer to [14] and the multimedia attachment.

Kinematics Model: The WIHM kinematics provide a mapping between the actuator space, the finger space and the object pose in the Cartesian space. Our mechanism is a switching system; the motion of the object depends on the finger friction configuration, and we derive a kinematics model for each of the above-mentioned $\{$*left finger*, *right finger*$\}$ configurations. The model variables d_L, d_R, θ_L and θ_R are depicted in Fig. 2 for the case of the object sliding along the right finger. Here, d_L is the distance from the left finger joint to the object's bottom corner and d_R is the distance from the right finger joint to the object's bottom corner. θ_L and θ_R are the angles of the fingers. When the object slides, one of its surfaces maintains contact with the high-friction surface while the opposite surface slides against the low-friction finger. This constraint of the object being effectively stationary against one finger is used to find the position of the object center as follows (for sliding against the right finger case):

$$\begin{bmatrix} x \\ y \end{bmatrix} = \begin{bmatrix} (d_L + b)cos(\theta_L) + (a + f_w)sin(\theta_L) \\ (d_L + b)sin(\theta_L) - (a + f_w)cos(\theta_L) \end{bmatrix} \tag{1}$$

A similar approach can be followed to derive the kinematics model for sliding along the other finger. The velocity of the object while sliding on the right finger can be obtained by differentiating Eq. (1) with respect to time. After simplifying the equation and using Eq. (1) we get,

$$\begin{bmatrix} \dot{x} \\ \dot{y} \end{bmatrix} = \begin{bmatrix} -y \\ x \end{bmatrix} \dot{\theta}_L \tag{2}$$

We observe that the Jacobians for the sliding motion on the left and the right finger are independent of the variables $d_L, d_R, \theta_L, \theta_R$ and the dimensions of the object.

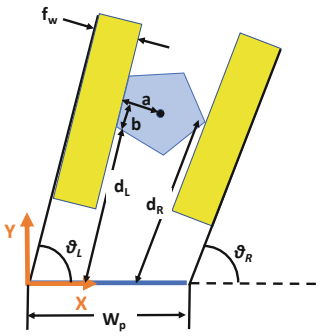

Fig. 2. Parameters of the kinematic model for the hand-object system

These equations are utilized to derive the planning and control schemes while also considering the non-holonomic and switching nature of the hand. We propose three approaches: a feedforward control method based on an WIHM planner, a feedback control method using a visual servoing scheme, and a hybrid method that combines these two methods.

WIHM Planner: For the WIHM planning problem, the state of the object is expressed in the finger space, i.e. $s = (d_L, d_R, \alpha)$, where α is the object orientation with respect to the finger. This provides an intuitive way to formulate cost functions for the actions (an alternative way would be to use the object pose in the Cartesian space, which has a one-to-one mapping to the finger space variables for the feasible object poses, and a very similar formulation would follow).

An A* planning framework is adopted to find the sequence of actions that leads the object to any target pose. The actions are defined as A = (slide_up_on_left_finger, slide_up_on_right_finger, slide_down_on_left_finger, slide_down_on_right_finger, rotate_left, rotate_right). We prefer to obtain a path with few friction state switches, since frequent switching results in non-smooth trajectories and increases the execution time. Applying the conventional A* algorithm to our problem generates a sequence of actions connecting the start state to the goal state with the lowest possible cost. The cost is given by

$$f(s') = g(s') + h(s') \tag{3}$$

where s' is the next state after an action is executed, $f(s')$ is the estimated cost from the start state to goal state, through s'. $g(s')$ is the accumulated cost, and $h(s')$ is the estimated cost to reach goal state from s' (Manhattan distance towards the goal). The trajectory generated using this formulation could (and often does) result in chattering, which means the sliding actions need to switch between the left and right fingers frequently in order to reach the goal position in the shortest possible way. Such chattering is highly undesired for our system, since it requires frequent switching between finger modes (i.e.

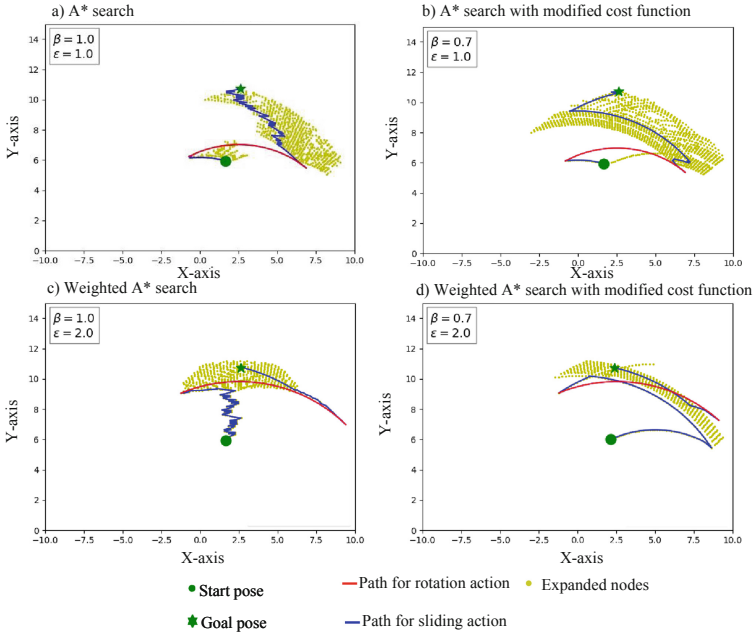

Fig. 3. Path generated by different A* searches

$\{high\_friction, low\_friction\}$ to $\{low\_friction, high\_friction\}$ and vice versa), which does not only take time, but also causes wear and tear of the hardware. Smooth paths can be achieved by relaxing the optimality constraint, and balancing between the path smoothness and the path length. This is achieved by assigning low costs to nodes which are expanded by the same action as their parent node. We define the heuristic cost $h(s)$ of a node as follows:

$$h(s) = \beta * h(s) \tag{4}$$

where

$$\beta = \begin{cases} 0 < \beta < 1, & \text{if } a == P_a \\ 1, & \text{otherwise} \end{cases} \tag{5}$$

In these equations, a is the action of the current node and P_a is the action of the parent node. The modified heuristic cost function makes the algorithm choose a smoother trajectory by favoring the parent node action, sometimes at the expense of not obtaining the shortest path. Figure 3-a presents the unmodified heuristic, and Fig. 3-b shows the trajectory with the modified heuristic. It can be observed that the path is smoother with the modified heuristic, but the number of nodes expanded are more than unmodified heuristic which makes the search algorithm significantly slower.

Therefore, we implement a weighted A* algorithm with a scaled heuristic similar to [8]:

$$f(s) = g(s) + \epsilon * h(s) \qquad where\ \epsilon > 1 \tag{6}$$

The ϵ parameter creates a bias for expanding more nodes closer to the goal, which speeds up the search (Fig. 3-c). The combination of the modified heuristic and weighted A* generates smooth paths with shorter amount of time (Fig. 3-d) compared to the classical formulation.

Visual Servoing for WIHM:

A position-based visual servoing method is designed as follows: We decompose the task into orientation correction and position correction in the finger space. We correct the positioning errors by sliding the object either along the left finger or along the right finger. We derive separate Jacobians for each of these finger friction states, and in each time step, we calculate both of the Jacobians, calculate associated object velocity vectors, and choose the one that is closest to the optimal path in the image space (i.e. a linear path).

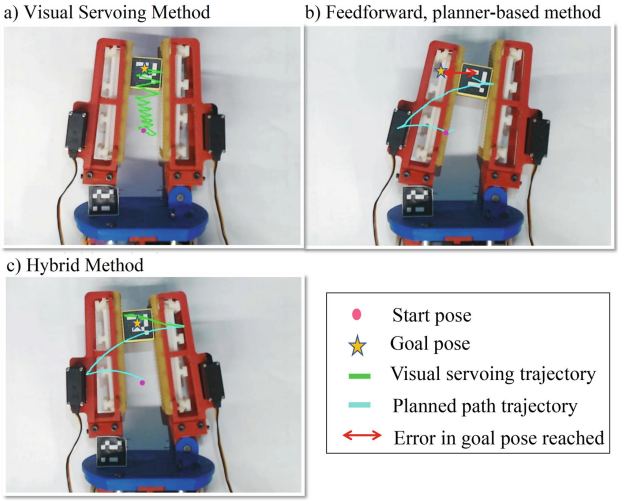

Fig. 4. Trajectory of the object from start pose to goal pose for the proposed three methods (only position correction case).

A complete rotation of the object (e.g. 90° for a rectangular prism) cannot be initiated from all points in the workspace, since this action requires large object displacements that may lead the object to the workspace limits. The motion planner finds a path that brings the object to a location where rotation is feasible, but visual servoing algorithm is essentially a local optimizer, and lacks the mechanisms to do so. In order to overcome this disadvantage, we first move the system close to the edges of the workspace, where rotations can easily be conducted (right-side edge for clockwise rotation and left-side edge for anti-clockwise rotation of the object), and then execute the rotation action. These locations are predetermined and hard-coded. Once the rotation is corrected, we continue executing position correction steps. The object trajectories obtained with this strategy may end up being far from optimum. Nevertheless, combining the offline planner and the visual servoing algorithm provides an alternative solution as follows.

The Hybrid Method: Executing the path of the offline motion planner directly on the real hardware results in significant inaccuracies (as shown in the Fig. 4-b) mainly due to the inaccuracies of the hand-object model. While utilizing vision feedback can make the system robust to these inaccuracies, using it in a standalone manner may not be preferable either since 1) we need to utilize some rules to manage the discrete rotation motions, which results in far-from-optimal trajectories, 2) high frequency chattering happen during convergence (Fig. 4-a). Therefore, we propose a hybrid controller, in which the offline planner generates 'via points', and the visual servoing algorithm tracks these intermediate goals in a close loop system. Such an approach results in both smooth and accurate WIHM Fig. 4-c. In the next sections, we analyze the performance of the motion planner, the pure visual servoing approach and the hybrid approach with experiments.

3 Experiments and Results

We conducted experiments with the setup presented in Fig. 5. The support plane below the object is removed after the initial grasp is achieved so that the WIHM is conducted in the air. To simplify the object tracking aspect and to focus on the controller performances, we used ArUco markers and the associated tracking packages [6]. We conducted experiments with all three control methods (feedforward, feedback and hybrid) using five different objects shown in Fig. 6. Four goal poses are generated: *goal-1* which requires only position correction, *goal-2* which requires position correction and one clockwise rotation, *goal-3* which requires position correction with one anti-clockwise rotation, and *goal-4* which requires position correction with two clockwise rotations. Here, we define "one rotation" as switching the contact to the adjacent edge of the object. For example, for the square prism, one rotation means a 90-degree rotation with respect to the finger surface. In our experiments, these discrete rotation references are always achieved reliably. Therefore, we do not report rotation errors since they are all zero.

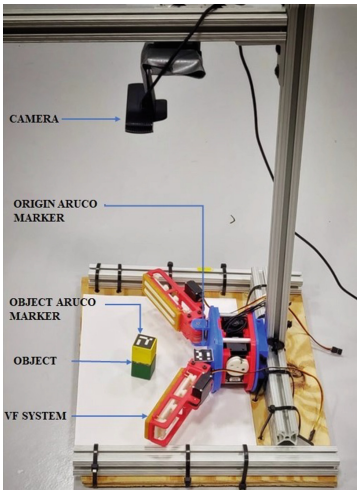

Fig. 5. The experimental setup.

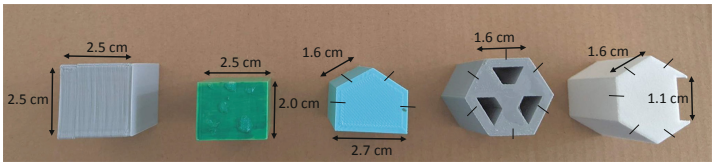

Fig. 6. Objects used in the experiments

The results with different object geometries are summarized in Table 1 (5 objects × 3 methods × 4 goals = 60 experiments total). The planner provides the most optimal path with the least number of switching, and takes the least amount of time to execute the task. However, it results in significant steady state error due to the modeling inaccuracies. Visual servoing method results in accurate positioning, but has longer execution time due to the increased switching and relatively inefficient rotation strategy. The hybrid method combines the advantages of the planner and visual servoing; it provides an accurate and efficient strategy for WIHM.

Using only the square object, we also conducted 20 experiments with each method with randomly generated goal poses (60 experiments) in order to identify any failure modes. The system was successfully able to conduct all the tasks. The results are summarized in Table 2. These results show very similar characteristics to the previous set of experiments.

In addition, we apply the *goal-4* reference 10 times repeatedly to each method using the square prism in order to study the repeatability of each method. From the results are shown in Table 3, we observe that the feedforward motion planner-based method show a high standard deviation, whereas feedback methods keep the error low consistently. The transient behavior show relatively minor fluctuations for all three methods.

Finally, in order to analyze each method's robustness to modeling inaccuracies, we also conducted experiments with the square prism object by introducing 20% error for the object size in the model. The results are presented in Table 4. The feedforward controller performance drops in terms of accuracy, path length and execution time. The visual servoing and hybrid methods generally maintained their performance.

Table 1. Averaged results for experiments with 5 different objects and 4 different goals

	Error (cm)	Switching Actions	Path length (cm)	Time Taken (s)
Motion Planner	1.21 ± 0.55	4.11 ± 0.97	24.52 ± 4.54	24.88 ± 3.65
Visual Servoing	0.41 ± 0.04	6.36 ± 1.19	28.11 ± 6.21	30.15 ± 3.70
Hybrid	0.38 ± 0.05	5.13 ± 1.08	26.76 ± 4.36	28.77 ± 3.88

Table 2. Results with square prisms with 20 randomly generated goals

	Error (cm)	Switching Actions	Path length (cm)	Time Taken (s)
Motion Planner	1.38 ± 0.57	4.35 ± 0.87	21.66 ± 5.42	25.30 ±2.49
Visual Servoing	0.39 ± 0.09	6.15 ± 0.74	27.73 ± 7.51	30.8 ± 3.27
Hybrid	0.37 ± 0.03	5.65 ± 0.98	26.51 ± 5.28	27.99 ± 4.62

Table 3. Results using square prisms with *goal*-4 as the desired pose

	Error (cm)	Switching Actions	Path length (cm)	Time Taken (s)
Motion Planner	1.29 ± 0.43	5.00 ± 0.0	23.54 ± 3.71	27.31 ± 2.03
Visual Servoing	0.41 ± 0.05	5.90 ± 0.38	27.96 ± 4.34	33.12 ± 3.01
Hybrid	0.38 ± 0.09	5.50 ± 0.40	25.92 ± 4.20	32.78 ± 3.17

Table 4. Summary of experiments with square prism focusing on modeling inaccuracies

	Error (cm)		Switching Actions		Path length (cm)		Time taken (s)	
	Correct Object Size	Wrong Object Size	Correct Object Size	Wrong Object Size	Correct Object Size	Wrong Object Size	Correct Object Size	Wrong Object Size
Motion Planner	1.16 ± 0.63	1.97 ± 0.29	4.25 ± 0.95	4.25 ± 0.95	20.54 ± 6.20	23.13 ± 6.96	24.25 ± 4.99	25.5 ± 4.57
Visual Servoing	0.40 ± 0.05	0.36 ± 0.03	5.75 ± 1.50	7.75 ± 0.5	26.52 ± 6.21	26.16 ± 9.66	32.25 ± 4.57	30.00 ± 9.12
Hybrid	0.29 ± 0.09	0.15 ± 0.08	5.75 ± 1.25	5.5 ± 1.73	26.56 ± 6.95	25.59 ± 9.56	29.00 ± 7.12	34.75 ± 4.27

4 Experimental Insights and Conclusions

It is important to note that the presented WIHM tasks achieved with our hand and the proposed controllers are beyond the capabilities of any other within-hand manipulation system in literature; to the best of our knowledge, there does not exist any other system that can automatically conduct controlled within-hand sliding and large rotations without heavily relying on accurate models. The systems in [7,10,11,16] are mechanically capable of similar actions, but no automatic WIHM schemes are proposed for those hands. Nevertheless, we believe that the controllers proposed in this work can easily be adopted to such systems.

Our experimental results show that each method has its advantages and disadvantages and can be utilized for different purposes. The feedforward method can be used in cases when smooth and fast executions are required and when the accuracy is not a major concern. Visual servoing algorithm can provide high-accuracy without requiring any planning, but it can cause chattering (since it tries to follow a straight path with the non-holonomic system), and its orientation

correction strategy is inefficient. The hybrid method requires planning, but can provide smooth trajectories and accurate results. Some of these aspects can be observed in the sample trajectories in Fig. 4.

The model knowledge required by our system is simpler than the conventional methods. We do not need to know friction coefficients between the object and the fingers; the mechanism with interlaced high- and low-friction surfaces can achieve controlled sliding and rotation for a large family of objects. Our system works in the quasi-static level, therefore does not require any dynamics model. The experiments with erroneous kinematic models (Table 4) shows that the closed loop algorithms are robust to kinematic model inaccuracies as well. We believe that the proposed algorithms and the presented results strongly indicate the importance of integrating variable friction context to the planning and control scheme for reliable and robust WIHM.

References

1. Bullock, I.M., Dollar, A.M.: Classifying human manipulation behavior. In: International Conference on Rehabilitation Robotics, pp. 1–6 (2011)
2. Calli, B., Dollar, A.M.: Robust precision manipulation with simple process models using visual servoing techniques with disturbance rejection. IEEE Trans. Automat. Sci. Eng. **16**(1), 406–419 (2018)
3. Calli, B., Kimmel, A., Hang, K., Bekris, K., Dollar, A.: Path planning for within-hand manipulation over learned representations of safe states. In: International Symposium on Experimental Robotics (ISER) (2018)
4. Chong, N.Y., Choi, D., Suh, I.H.: A generalized motion/force planning strategy for multifingered hands using both rolling and sliding contacts. In: IEEE/RSJ International Conference on Intelligent Robots and Systems, pp. 113–120 (1993)
5. Dafle, N.C., Rodriguez, A., Paolini, R., Tang, B., Srinivasa, S.S., Erdmann, M., Mason, M.T., Lundberg, I., Staab, H., Fuhlbrigge, T.: Extrinsic dexterity: In-hand manipulation with external forces. In: IEEE International Conference on Robotics and Automation (ICRA), pp. 1578–1585. IEEE (2014)
6. Garrido-Jurado, S., Muñoz-Salinas, R., Madrid-Cuevas, F.J., Marín-Jimínez, M.J.: Automatic generation and detection of highly reliable fiducial markers under occlusion. Pattern Recogn. **47**(6), 2280–2292 (2014)
7. Govindan, N., Thondiyath, A.: Design and analysis of a multimodal grasper having shape conformity and within-hand manipulation with adjustable contact forces. J. Mech. Robot. **11**(5), 051012 (2019)
8. Hansen, E.A., Zhou, R.: Anytime heuristic search. J. Artif. Int. Res. **28**(1), 267–297 (2007)
9. Karayiannidis, Y., Pauwels, K., Smith, C., Kragic, D., et al.: In-hand manipulation using gravity and controlled slip. In: IEEE/RSJ International Conference on Intelligent Robots and Systems, pp. 5636–5641 (2015)
10. Lu, Q., Clark, A.B., Shen, M., Rojas, N.: An origami-inspired variable friction surface for increasing the dexterity of robotic grippers. IEEE Robot. Automat. Lett. **5**(2), 2538–2545 (2020)
11. Nojiri, S., Mizushima, K., Suzuki, Y., Tsuji, T., Watanabe, T.: Development of contact area variable surface for manipulation requiring sliding. In: IEEE International Conference on Soft Robotics, pp. 131–136 (2019)

12. Salisbury, J.K., Mason, M.: Robot Hands and the Mechanics of Manipulation. MIT Press, Cambridge (1985)
13. Shi, J., Woodruff, J.Z., Umbanhowar, P.B., Lynch, K.M.: Dynamic in-hand sliding manipulation. IEEE Trans. Rob. **33**(4), 778–795 (2017)
14. Spiers, A.J., Calli, B., Dollar, A.M.: Variable-friction finger surfaces to enable within-hand manipulation via gripping and sliding. IEEE Robot. Automat. Lett. **3**(4), 4116–4123 (2018)
15. Sundaralingam, B., Hermans, T.: Relaxed-rigidity constraints: kinematic trajectory optimization and collision avoidance for in-grasp manipulation. Auton. Robot. **43**(2), 469–483 (2019)
16. Tincani, V., Grioli, G., Catalano, M.G., Garabini, M., Grechi, S., Fantoni, G., Bicchi, A.: Implementation and control of the velvet fingers: a dexterous gripper with active surfaces. In: IEEE International Conference on Robotics and Automation, pp. 2744–2750 (2013)
17. Ueda, J., Kondo, M., Ogasawara, T.: The multifingered naist hand system for robot in-hand manipulation. Mech. Mach. Theory **45**(2), 224–238 (2010)